Diagnostic approach to the anterior/prevascular mediastinum for radiologists

Brett W. Carter[1], Marcelo F. Benveniste[1], Edith M. Marom[2]

[1]Department of Diagnostic Radiology, The University of Texas MD Anderson Cancer Center, Houston, TX, USA; [2]Department of Radiology, Chaim Sheba Medical Center, Affiliated with the University of Tel Aviv, Tel Aviv, Israel
Contributions: (I) Conception and design: All authors; (II) Administrative support: None; (III) Provision of study materials or patients: None; (IV) Collection and assembly of data: None; (V) Data analysis and interpretation: None; (VI) Manuscript writing: All authors; (VII) Final approval of manuscript: All authors.
Correspondence to: Brett W. Carter, MD. The University of Texas MD Anderson Cancer Center, Department of Diagnostic Radiology, 1515 Holcombe Blvd., Unit 1478, Houston, TX 77030, USA. Email: bcarter2@mdanderson.org.

Abstract: The mediastinum contains vital vascular and nonvascular organs and other structures, and a wide variety of neoplasms and other abnormalities may originate from this anatomic region of the chest. Division of the mediastinum into distinct compartments helps narrow the differential diagnosis of mediastinal abnormalities detected on imaging studies, assists the planning of biopsy and surgical procedures, and facilitates communication between healthcare providers in the multidisciplinary setting. Numerous different models have been developed and used by radiologists, surgeons, and anatomists. Recently, the International Thymic Malignancy Interest Group (ITMIG) developed a new classification model of the mediastinal compartments based on cross-sectional imaging that has been accepted as a new standard. Although mediastinal pathology may be first identified on chest radiographs, cross-sectional imaging techniques such as computed tomography (CT) and magnetic resonance (MR) imaging play critical roles in the identification, localization, and characterization of mediastinal lesions. CT is considered the imaging modality of choice to evaluate most masses; however, MR imaging is superior to CT in differentiating between cystic and solid lesions, identifying cystic and solid components within complex masses, and distinguishing thymic hyperplasia and normal thymus from thymic epithelial neoplasms and other neoplasms. In this article, the new ITMIG classification of mediastinal compartments is presented along with approaches to the imaging evaluation of masses in the anterior/prevascular mediastinum.

Keywords: Mediastinum; imaging; computed tomography (CT); magnetic resonance imaging (MR imaging); International Thymic Malignancy Interest Group (ITMIG)

Introduction

The mediastinum contains vital vascular and nonvascular organs and other structures, and a wide variety of neoplasms and other abnormalities may originate from this anatomic region of the chest. Localization of mediastinal abnormalities, which may be neoplastic, congenital, vascular, or lymphatic in etiology, to specific compartments has traditionally been beneficial for the characterization of these lesions, providing guidance for further patient management including additional imaging examinations, biopsies, and surgical procedures, if necessary. Several different classification systems have been developed and utilized by anatomists, surgeons, and radiologists to varying degrees. The Shields classification system is the most commonly used scheme in clinical practice, and traditional Fraser and Paré, Felson, Heitzman, Zylak, Whitten, and other models have been used by radiologists

(1-8). However, significant differences in the methods of compartmentalization and the terminology used in these systems have resulted in confusion and miscommunication between healthcare providers evaluating patients with mediastinal abnormalities.

Most of the mediastinal compartment models used in radiologic practice represent arbitrary divisions of the chest based on the lateral chest radiograph that are non-anatomic. A standardized classification scheme based on cross-sectional imaging, including computed tomography (CT), magnetic resonance (MR) imaging and fluorodeoxyglucose (FDG) positron emission tomography (PET)/CT, has been necessary as these techniques are those typically employed to evaluate and diagnose mediastinal abnormalities. This has become particularly important given the growing number of lesions detected with CT performed for lung cancer screening, cardiac screening, and other purposes (9,10). The Japanese Association for Research on the Thymus (JART) developed a CT-based 4-compartment model from a retrospective study of 445 nonconsecutive pathologically proved mediastinal masses that was published in 2014 (11). Increased interest in the mediastinum and disease processes that may be found there, particularly thymic epithelial neoplasms, has led to greater international collaboration and ultimately resulted in the formation of the International Thymic Malignancy Interest Group (ITMIG). This multidisciplinary organization provides an infrastructure for studying the mediastinum and, with the formation of an international thymic malignancy database, it is hoped that large-scale multi-institutional studies will continue to advance the scientific knowledge of these tumors and other lesions. Since its inception, ITMIG has crafted and published numerous standards and policy papers, guidelines, and recommendations addressing specific topics, knowledge gaps, and limitations of existing guidelines. ITMIG modified the JART model and introduced a new definition of mediastinal compartments to be used with cross-sectional imaging that has been accepted as a new standard (12).

Imaging plays a critical role in the management of patients with mediastinal masses, as it enables localization and characterization of lesions, facilitates the generation of focused differential diagnoses and ultimately guides clinical management. In some cases, specific imaging characteristics may be seen within mediastinal masses that suggest a specific diagnosis; in other instances, a combination of radiologic and clinical information is necessary to determine the next step in management. In this article, the new ITMIG mediastinal compartment classification system based on cross-sectional imaging is presented along with specific approaches to the evaluation of abnormalities in the prevascular compartment are presented. These approaches are not intended to include every possible entity that may be encountered in this region of the mediastinum but provide a practical and realistic algorithm for the radiologist to use in clinical practice.

ITMIG definition of mediastinal compartments

The ITMIG system separates the mediastinum into prevascular (anterior), visceral (middle), and paravertebral (posterior) compartments (*Table 1*). The boundaries of these compartments and the anatomic structures they contain can be identified on cross-sectional imaging.

Prevascular compartment

The boundaries of the prevascular compartment include: (I) superiorly—the thoracic inlet; (II) inferiorly—the diaphragm; (III) anteriorly—the posterior border/cortex of the sternum; (IV) laterally—the parietal mediastinal pleura; and (V) posteriorly—the anterior aspect of the pericardium (*Table 1*). As the thymus, fat, lymph nodes, and the left brachiocephalic vein are present in the prevascular compartment, the most common abnormalities encountered in this region include thymic lesions (cysts, hyperplasia, and thymic epithelial neoplasms including thymoma, thymic carcinoma, and thymic carcinoid), germ cell neoplasms, lymphoma, metastatic disease, and goiter.

Visceral compartment

The boundaries of the visceral compartment include: (I) superiorly—the thoracic inlet; (II) inferiorly—the diaphragm; (III) anteriorly—the posterior boundaries of the prevascular compartment; and (IV) posteriorly—a vertical line connecting a point on the thoracic vertebral bodies 1 cm posterior to the anterior margin of the spine (referred to as the visceral-paravertebral compartment boundary line) (*Table 1*). Vascular structures such as the heart, superior vena cava, thoracic aorta, intrapericardial pulmonary arteries, and the thoracic duct, and non-vascular structures including the trachea, carina, esophagus, and lymph nodes, can be found in this compartment. All structures enclosed by the pericardium are present in the visceral compartment whereas the extrapericardial pulmonary arteries and veins are considered pulmonary structures and

Table 1 ITMIG classification of mediastinal compartments

Compartment	Boundaries	Major contents
Prevascular	Superior: thoracic inlet	Thymus
	Inferior: diaphragm	Fat
	Anterior: sternum	Lymph nodes
	Lateral: parietal mediastinal pleura	Left brachiocephalic vein
	Posterior: anterior aspect of the pericardium as it wraps around the heart in a curvilinear fashion	
Visceral	Superior: thoracic inlet	Non-vascular: trachea, carina, esophagus, lymph nodes
	Inferior: diaphragm	Vascular: heart, aorta, superior vena cava, intrapericardial pulmonary arteries, thoracic duct
	Anterior: posterior boundaries of the prevascular compartment	
	Posterior: vertical line connecting a point on each thoracic vertebral body at 1 cm posterior to its anterior margin	
Paravertebral	Superior: thoracic inlet	Thoracic spine
	Inferior: diaphragm	Paravertebral soft tissues
	Anterior: posterior boundaries of the visceral compartment	
	Posterolateral: vertical line against the posterior margin of the	
	chest wall at the lateral margin of the transverse process of the thoracic spine	

ITMIG, International Thymic Malignancy Interest Group.

are excluded. Lymphadenopathy (representing lymphoma or metastatic disease), duplication cysts, esophageal lesions, and cardiovascular abnormalities are responsible for most lesions found in the visceral compartment.

Paravertebral compartment

The boundaries of the paravertebral compartment include: (I) superiorly—the thoracic inlet; (II) inferiorly—the diaphragm; (III) anteriorly—the posterior boundaries of the visceral compartment; and (IV) posterolaterally—a vertical line along the posterior margin of the chest wall at the lateral aspect of the transverse processes (*Table 1*). As the thoracic spine and paravertebral soft tissues are the main structures found in this region, neurogenic neoplasms that arise from the dorsal root ganglia/neurons adjacent to the intervertebral foramina comprise most lesions in the paravertebral compartment. Other lesions abnormalities include discitis/osteomyelitis, hematoma, and miscellaneous conditions such as extramedullary hematopoiesis.

Imaging of mediastinal abnormalities

General considerations

More than half of all mediastinal masses arise from the anterior/prevascular compartment (10,13-21). In many cases, the localization of a lesion to a specific compartment and its detailed characterization on CT is sufficient to make the diagnosis or provide a focused differential diagnosis. However, in other instances, the CT findings may be nonspecific and correlation between imaging findings and clinical history, as well as additional imaging examinations such as MR imaging and PET/CT and histologic sampling through image-guided or surgical biopsy, may be necessary to make a definitive diagnosis and guide further management.

Radiography

As chest radiography remains the most commonly performed imaging examination, it may be the first

modality to demonstrate mediastinal pathology. Small mediastinal masses may not be visible or result in only subtle radiographic findings. Large lesions may result in a focal opacity or abnormalities involving the mediastinal lines, stripes, and interfaces. The lateral chest radiograph is beneficial for demonstrating abnormalities in the retrosternal space or overlying the upper thoracic spine which may not be visible on the posteroanterior radiograph. There are multiple signs which have been described on chest radiographs that can be useful in suggesting the presence of a mediastinal abnormality. One of these signs is known as the silhouette sign, and describes the loss of normal borders of intrathoracic structures. For example, a mass in the left anterior mediastinum may obscure the left heart border. Another helpful sign is the hilum overlay sign, which may help differentiate a mediastinal lesion from other abnormalities such as cardiomegaly or enlarged pulmonary vessels.

CT

The imaging modality of choice for identifying, localizing, and characterizing most mediastinal masses is CT. A study of 127 prevascular mediastinal masses of various etiologies by Tomiyama and colleagues showed that CT was equal or superior to MR imaging in correctly diagnosing most of the lesions, except for thymic cysts (22). Specific information that should be identified on CT and reported in the clinical report include the following: (I) location, size, morphology, shape, and margins; (II) density, heterogeneity and enhancement; (III) fat, cystic components, soft tissue, and calcification; and (IV) connection with or invasion of adjacent structures. Although all of these features are important for thorough characterization, some of them are more diagnostically relevant than others. As an example, the presence of fat in a prevascular mediastinal mass on CT narrows the differential diagnosis considerably, and includes lesions such as mature teratoma, thymolipoma, and, less commonly, lipoma and liposarcoma. In contrast, calcifications are nonspecific and may be associated with benign or malignant mediastinal lesions.

MR imaging

MR imaging is not routinely performed to evaluate all mediastinal masses; however, it is the best modality for distinguishing cystic from solid masses (e.g., thymic cysts from solid tumors), identifying cystic and/or necrotic components within solid lesions, demonstrating septations and/or soft tissue within cystic lesions, and distinguishing thymic hyperplasia and normal thymus from soft tissue tumors. A variety of MR imaging protocols have been developed to evaluate the mediastinum, most of which include T1-weighted, T2-weighted, T2-weighted fat-saturated, in-phase and out-of-phase gradient echo (GRE), and pre- and post-gadolinium enhanced sequences (23,24). Diffusion weighted imaging (DWI), dynamic contrast enhanced (DCE) imaging, and short tau inversion recovery (STIR) sequences may also be performed and have been shown to add value. Although breath hold or respiratory gating techniques may be utilized, the former is usually preferred given its greater reliability in halting respiratory motion and preventing artifacts. Cardiac gating can be achieved with either electrocardiogram (ECG) gating or peripheral gating, the former of which is preferred due to more reliable halting of cardiac motion and elimination of pulsatility artifacts (23,24).

The presence of microscopic or intravoxel fat is best evaluated with chemical shift imaging which includes in-phase and out-of-phase GRE sequences. Thymic hyperplasia may manifest as a focal soft tissue mass in the prevascular mediastinum and mimic soft tissue neoplasms such as thymic epithelial tumors; however, chemical shift imaging can distinguish between these entities, as thymic hyperplasia and normal thymus lose signal on out-of-phase sequences due to the suppression of microscopic fat interspersed between non-neoplastic thymic tissue whereas soft tissue neoplasms do not (25-27). A specific chemical shift ratio (CSR) has been described that can calculate the signal loss, in which CSR = (thymus SI OP/paraspinal muscle SI OP)/(thymus SI IP/paraspinal muscle SI IP), in which SI = signal intensity, IP = in-phase sequences, and OP = out-of-phase sequences. Thymic hyperplasia and normal thymus typically show CSRs of 0.5–0.6. In contrast, thymic epithelial neoplasms, lymphoma, and other soft tissue neoplasms exhibit CSRs of 0.9–1.0 (25-27). Recently, a simpler equation, the signal intensity index (SII) showed better differentiation between thymic hyperplasia and malignancy, in which SII = [(thymus SI IP – thymus SI OP)/thymus SI IP] ×100 (28). Values reached are the percentage of signal drop on out of phase images. Values higher than 9% signal drop were only seen in thymic hyperplasia, which usually manifests with a 28–65% signal drop on out of phase imaging. Of malignant lesions that show a signal drop on out of phase imaging, the signal drop was usually less than 5%.

DWI and DCE imaging have shown promise in early studies in differentiating between types of thymoma and other types of prevascular mediastinal masses. In one study, an apparent diffusion coefficient (ADC) value of 1.56×10^{-3} mm^2/s was found to have 96% sensitivity, 94% specificity, and 95% accuracy for differentiating between malignant and benign mediastinal masses (29). Benveniste and colleagues evaluated 38 mediastinal masses with DWI and found that a mean ADC value was statistically significant in differentiating benign from malignant masses, benign thymic lesions from thymic epithelial neoplasms, and thymic epithelial neoplasms from non-thymic mediastinal neoplasms (30). However, differentiation between low-grade thymomas, high-grade thymomas and thymic carcinomas and early from late stage thymomas with ADC values was not possible. Sakai and colleagues evaluated 59 patients with sequential imaging at 30 seconds for 5 minutes following the administration of IV gadolinium contrast material and reported that low-risk thymomas (Masaoka stages I and II) showed rapid time-to-peak enhancement with a mean time of 1.5 minutes (31). In contrast, the mean time to peak enhancement for stage III thymomas was 2.5 minutes. Other etiologies such as thymic carcinoma, lymphoma, malignant germ cell tumor and thymic carcinoid demonstrated gradual enhancement over time with a mean time-to-peak enhancement of 3.2 minutes. A threshold value of 2 minutes to peak enhancement enabled differentiation between low-risk thymomas from these other neoplasms with 81% accuracy.

Finally, MR imaging can assist in the staging and evaluation of treatment response of patients with thymic epithelial tumors and other neoplasms in whom iodinated IV contrast material is contraindicated due to severe allergy and/or impaired renal function. Such patients should undergo MR imaging with specific fluid-sensitive sequences, not unenhanced chest CT. This is important particularly prior to therapy to evaluate for involvement of the cardiac and/or vascular structures, which typically necessitates the administration of neoadjuvant therapy in the case of thymic epithelial neoplasms (25).

FDG PET/CT

The role of FDG PET/CT in the evaluation and characterization of mediastinal abnormalities is controversial. One of the most significant limitations of FDG PET/CT is that infections and other non-neoplastic disease processes such as thymic hyperplasia and fibrosing mediastinitis resulting in mediastinal inflammation may demonstrate increased FDG uptake and result in false positive interpretation. Jerushalmi and colleagues showed that FDG uptake in thymic hyperplasia is highly variable and in can significantly overlap with that of mediastinal malignancies, with SUVmax as high as 7.3 (32). Thus, a combination of clinical history, focality of FDG uptake at PET/CT, and morphologic features on CT is necessary to determine whether the lesion is benign or malignant.

Multiple studies have been performed to investigate its ability to differentiate between malignant and benign lesions and between specific types of malignant tumors. In one study, Kubota *et al.* evaluated 22 patients with primary mediastinal tumors (33). The mean FDG uptake of malignant neoplasms was significantly higher than that of benign tumors. High FDG uptake (defined as differential uptake value, or DUV, which is similar to SUV) was present in nine of ten patients with thymic carcinoma, lymphoma, and invasive thymoma, as well as a case of sarcoidosis; moderate FDG uptake (DUR >1.5) was seen in myeloma, noninvasive thymoma, and schwannoma; and low FDG uptake (DUR <1.5) was present in teratoma and benign cysts. The authors suggested that a cutoff value of 3.5 could be used to differentiate malignant from benign mediastinal lesions. In another study, Tatci and colleagues evaluated the efficacy of FDG PET/CT for the differentiation of malignant from benign mediastinal masses and neurogenic tumors of the chest wall (34). The sensitivity, specificity, accuracy, positive predictive value (PPV) and negative predictive value (NPV) in the detection of malignancy were 90%, 55.17%, 67%, 50.94% and 91.43%, respectively, and SUVmax, mean Hounsfield unit (HU) values and lesion size were higher in malignant cases (P<0.05). A threshold SUVmax of 4.67 was used as a cutoff for benign and malignant lesions. The mean SUVmax was significantly higher in invasive thymomas than those of non-invasive thymomas (P=0.029) and SUVmax and mean HU values were higher in solid benign lesions than those of cystic benign lesions (P<0.05). The limited specificity (55.17%) was attributed to high false-positive results caused from Castleman disease, benign neurogenic tumors, and thymic hyperplasia. The authors suggested that FDG PET/CT is complementary to CT and noted that histologic sampling is ultimately required to confirm findings identified on PET/CT.

Luzzi and colleagues reported significant overlap between FDG-avid neoplasms including high-risk thymic epithelial neoplasms (WHO types B2 and B3), lymphoma, paraganglioma, and nonseminomatous germ cell tumors
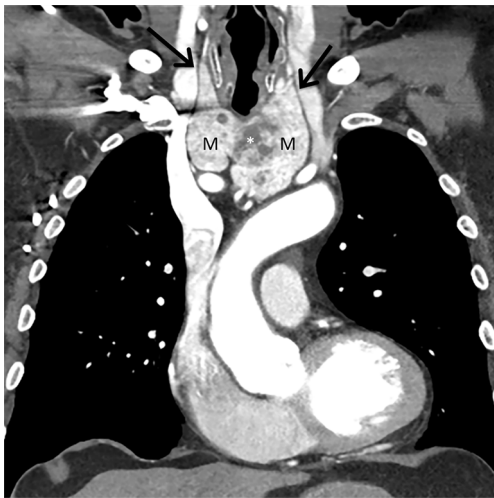
Figure 1 Thyroid goiter. Contrast-enhanced coronal CT of a 67-year-old woman demonstrates a large mass [M] in the prevascular mediastinum that is heterogeneous with regions of intense enhancement and low attenuation (asterisk). Note the connection with the cervical thyroid gland (arrows). These findings are consistent with intrathoracic extension of a goiter.

(NSGCTs) (35). Sung *et al.* suggested that PET/CT could be used to distinguish low-risk thymomas (WHO types A, AB, and B1) from thymic carcinoma and Treglia and colleagues have reported that FDG PET/CT could distinguish low-risk thymomas from high-risk thymomas (WHO types B2 and B3) and thymic carcinoma (36,37). Overall, it appears that the FDG PET/CT appearance of thymic epithelial neoplasms is variable and that lesions tend to demonstrate inconsistent FDG uptake with some lesions even demonstrating little to no FDG uptake. Additionally, other studies have demonstrated no clear benefit in staging with FDG PET/CT.

Localization of mediastinal masses

Localization of mediastinal abnormalities to specific compartments on imaging examinations is crucial; however, this may be difficult when large lesions involve multiple compartments or extend from one compartment to another. Two specific tools are recommended by ITMIG that may be helpful in lesion localization: (I) the "center method" and (II) the "structure displacement tool". The center method states that the center of a lesion, defined as its center point on the axial CT image on which the lesion has the greatest diameter, localizes the mass to a specific compartment.

When large lesions are present that displace organs from other mediastinal compartments, the structure displacement tool is particularly helpful. For instance, a very large visceral mediastinal mass may result in the anterior displacement of prevascular compartment structures such as the thymus or mediastinal fat.

Evaluation of the prevascular mediastinal compartment

The true incidence of prevascular mediastinal masses is difficult to establish for multiple reasons. The most significant confounding factor is the fact that different mediastinal division systems have been used in published studies (38). Another is the variability with which both non-neoplastic abnormalities such as thymic hyperplasia and thymic and pericardial cysts and other neoplastic lesions such as lymphoma have been included (and the nomenclature used) (38). The most common primary tumors of the prevascular mediastinal compartment include thymic epithelial neoplasms (thymoma, thymic carcinoma, and thymic neuroendocrine tumors) and lymphoma. Thymoma is the most common mass and primary neoplasm of the prevascular mediastinum, with the highest incidence in middle-aged patients. Mature teratoma, nonteratomatous germ cell malignancies such as seminoma and nonseminomatous germ cell neoplasms, and metastatic disease represent other benign and malignant neoplasms that may occur. Nonneoplastic lesions include substernal extension of thyroid goiter, thymic hyperplasia, cystic lesions such as thymic and pericardial cysts, and vascular-lymphatic abnormalities.

Evaluation based primarily on imaging findings

Thyroid goiter
Substernal extension of a thyroid goiter and an ectopic thyroid goiter occurring in the mediastinum manifest as heterogeneous prevascular mediastinal masses that demonstrate continuity with the cervical thyroid gland, are intrinsically hyperdense with HU values of 70–85 (due to the presence of iodine), and show intense and sustained enhancement following the administration of IV contrast (*Figure 1*). Internal regions of low density (due to cystic changes) and foci of high density (representing calcifications) may be present. Direct connection with the cervical thyroid gland is typically appreciable in the case of substernal extension. Additional findings such as loss of

mediastinal tissue planes and cervical and/or mediastinal lymphadenopathy should raise suspicion for thyroid malignancy (10,39).

Fat-containing masses

Several prevascular mediastinal masses manifest with

Figure 2 Mature teratoma. Contrast-enhanced axial CT of a 33-year-old man shows a heterogeneous mass [M] in the left prevascular mediastinum with macroscopic fat (asterisks), calcification (arrow), fluid, and soft tissue. When a mass containing these various elements is present in the prevascular mediastinum, the most likely diagnosis is a mature teratoma.

identifiable intralesional fat measuring between –40 and –120 HU on CT. The most common lesion is a mature teratoma, a benign germ cell neoplasm that typically demonstrates a combination of fat, fluid, calcification, and soft tissue (*Figure 2*). Bone and tooth-like elements have been reported within these lesions (40,41). Although one or more fat-fluid levels are highly specific for mature teratoma, this is much less common than gross macroscopic fat (42) (*Figure 3*). Mature teratoma represents 25% of prevascular masses in patients 10–19 years of age, 10–15% in patients 20–49 years of age, and less than 5% in patients over 50 years of age in both men and women (10).

Other fat-containing abnormalities in the prevascular mediastinum include neoplasms such as thymolipoma, lipoma, and liposarcoma and non-neoplastic abnormalities such as thymic hyperplasia. Thymolipoma is an uncommon lesion comprised of 50–95% adipose tissue and scattered regions of soft tissue and fibrous septa that represents less than 5% of prevascular mediastinal masses (41,43) (*Figure 4*). Thymolipomas usually occur in a cardiophrenic angle, grow very large (average reported size of 20 cm at presentation), and demonstrate a direct connection with the thymus. Patients may be asymptomatic or report clinical symptoms due to local mass effect. Associations between thymolipoma and myasthenia gravis, Graves' disease, and hematologic disorders have been reported but are rare (44). Lipoma is a benign neoplasm that represents 2% of all primary mediastinal tumors. On CT, lipomas manifest as encapsulated lesions composed principally of fat and a small
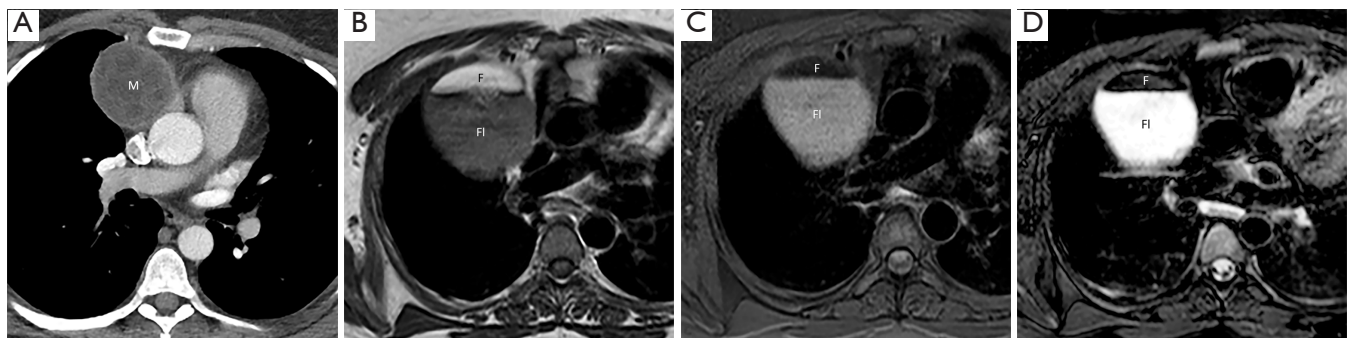

Figure 3 Mature teratoma. (A) Contrast-enhanced axial CT of a 40-year-old woman demonstrates a mass [M] in the right prevascular mediastinum with low attenuation due to a combination of fat and fluid. Although many teratomas contain a combination of fat, fluid, soft tissue, and calcification, some may demonstrate just fat and fluid. (B,C,D) Multiple MR images of a 43-year-old woman with a mature teratoma in the right prevascular mediastinum demonstrate the rare finding of a fat-fluid level. Axial T1-weighted MR image (B) shows high signal intensity fat [F] anteriorly and intermediate signal intensity fluid [Fl] posteriorly, the former of which loses signal on the axial T1-weighted fat saturated MR image (C) the and the latter of which demonstrates high signal intensity on the axial T2-weighted MR image (D). MR, magnetic resonance.

amount of soft tissue and blood vessels. Liposarcomas are malignant neoplasms that typically display aggressive features that can help distinguish them from lipomas, thymolipomas, and other fat-containing lesions such as a greater proportion of soft tissue components, local invasion, intrathoracic lymphadenopathy, and metastatic disease (45,46).

Cystic lesions

A variety of cystic lesions, defined as those that have water

Figure 4 Thymolipoma. Unenhanced axial CT of a 48-year-old man demonstrates a mass [M] in the left cardiophrenic sulcus primarily composed of fat with scattered regions of soft tissue and fibrous septa (arrow). Surgical resection was performed to relieve symptoms related to mass effect and thymolipoma was diagnosed.

or fluid density with HU values between 0 and 20 on CT, may be encountered in the prevascular mediastinum. One of the most common of these is a thymic cyst, which appears as a well-circumscribed homogeneous lesion near the thymic bed that is round, oval, or saccular in configuration. Thymic cysts may be congenital or acquired, the latter of which are much more common and are associated with inflammation; iatrogenic processes such as surgery, radiation therapy, or chemotherapy; and malignant neoplasms. Prevascular masses that are purely cystic based on HU values with no soft tissue components or internal septations most likely represent unilocular thymic cysts (47) (*Figure 5*). Other thymic cysts may demonstrate regions of much higher attenuation due to the presence of hemorrhagic or proteinaceous components. In this setting, MR imaging should be performed, as it is superior to CT in its ability to distinguish between cystic and solid lesions and identify cystic and solid internal components within complex lesions (*Figure 5*). Cystic lesions containing internal soft tissue components and/or internal septations include multilocular thymic cysts, cystic teratoma (*Figure 6*), lymphangioma, and cystic thymoma. In the clinical setting of symptoms related to myasthenia gravis or other paraneoplastic syndromes, especially in men and women older than 40 years, the diagnosis of cystic thymoma should be strongly considered.

In the setting of a large multilocular cystic lesion with internal septa and/or soft-tissue components that extends into the neck, axilla, or chest wall, the diagnosis of lymphangioma should be considered. Although mature teratomas may demonstrate internal fat at multidetector
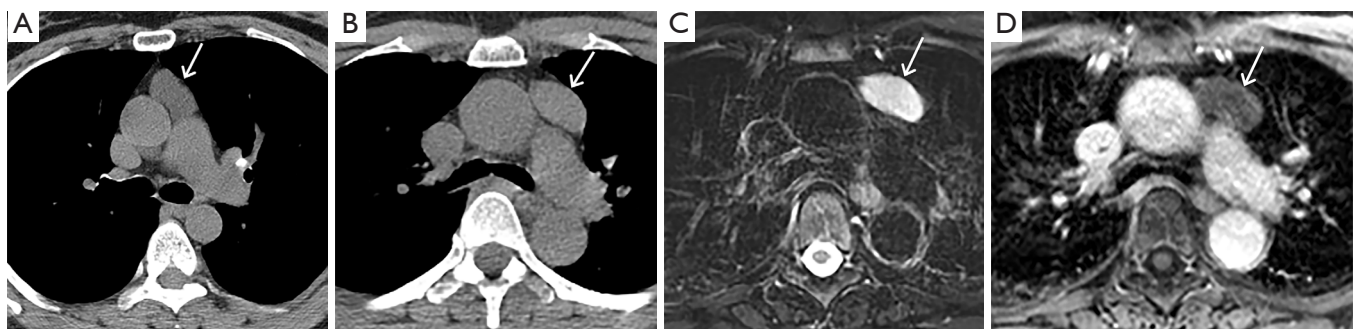

Figure 5 Thymic cyst. (A) Unenhanced axial CT of a 56-year-old woman shows a lobulated lesion (arrow) measuring fluid attenuation in the left prevascular mediastinum compatible with a thymic cyst. (B,C,D) CT and MR images of a 62-year-old woman with a thymic cyst. Unenhanced axial CT (B) demonstrates a lesion (arrow) in the left prevascular mediastinum that is of higher attenuation, similar in attenuation to the adjacent aorta and left pulmonary artery. Axial T2-weighted and contrast-enhanced T1-weighted MR images demonstrate high signal intensity within the abnormality (arrows) on the T2 weighted image (C) with and no enhancement after IV contrast injection (D), compatible with that of a thymic cyst with proteinaceous or hemorrhagic components. MR, magnetic resonance.
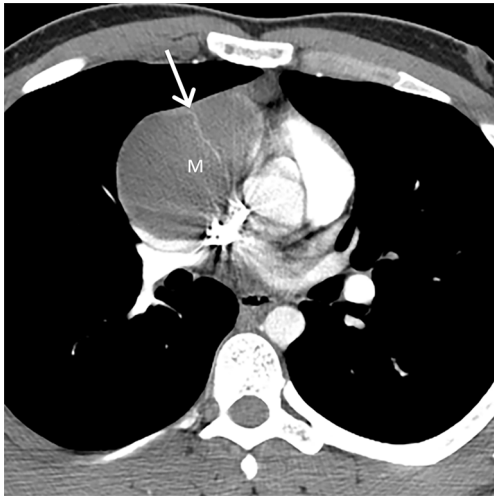
Figure 6 Cystic teratoma. Contrast-enhanced axial CT of a 19-year-old woman shows a predominantly low attenuation cystic mass [M] in the right prevascular mediastinum although an internal septation (arrow) is present. Surgical biopsy revealed cystic teratoma.

CT, a large percentage of these lesions manifest as predominantly or entirely unilocular or multilocular thin-walled cystic masses in the prevascular mediastinum. In contrast to simple cysts, cystic teratomas are typically associated with additional features such as internal septa and soft-tissue components and may enhance after administration of intravenous contrast material.

A well-circumscribed unilocular mass of fluid attenuation with thin or imperceptible walls localized to a cardiophrenic angle can be confidently diagnosed as a pericardial cyst. These benign nonneoplastic lesions arise from aberrations in the formation of coelomic or somatic cavities and more commonly arise in the right costophrenic angle than in the left, although they may be seen as high as the pericardial recesses at the level of the proximal aorta and pulmonary arteries (48). Although pericardial cysts are always connected to the pericardium, only a small number of cases demonstrate this communication at the time of surgery.

Evaluated based on a combination of imaging findings and clinical information

General considerations
Although CT findings may be sufficient to suggest a specific diagnosis or narrow the differential diagnosis for some prevascular mediastinal abnormalities, in other cases a combination of imaging and clinical information is necessary to guide further management. This is most common when prevascular masses are predominantly soft tissue, as several benign and malignant conditions can result in such an appearance.

Thymic hyperplasia
Normal thymic tissue is usually only observed in young patients and decreases with advancing age. Complete fatty replacement is typically seen by 40 years of age. In the setting of new uniform thymic enlargement or soft tissue with the normal bilobed triangular configuration, thymic hyperplasia should be strongly considered. True thymic hyperplasia, also known as "rebound hyperplasia," is defined as an increase in thymic volume of greater than 50% over baseline and affects patients who have been treated with chemotherapy, radiation therapy, or corticosteroids, or exposed to stresses such as burns or injuries. It is estimated that 10–25% of patients treated with chemotherapy develop thymic rebound hyperplasia (49). In these patients, CT demonstrates diffuse symmetric thymic enlargement. Thymic lymphoid (follicular) hyperplasia is characterized by an increased number of lymphoid follicles with or without an increase in gland size. Patients with immunologic diseases such as myasthenia gravis, hyperthyroidism, collagen vascular diseases, or human immunodeficiency virus (HIV) infection are typically affected and CT may demonstrate normal thymus, thymic enlargement, or a focal soft tissue mass (10). Rarely, thymic hyperplasia may appear as a heterogeneous mass with regions of low density due to deposition of fat between hyperplastic thymic tissue.

Thymic hyperplasia may manifest on CT with a nodular or bulky configuration and mimic soft tissue neoplasms such as thymic epithelial tumors, lymphoma, and others. In such cases, patients should undergo further imaging to avoid unnecessary biopsies or surgeries. One option is for patients to be re-evaluated with CT in 3 months, during which time a decrease in thymic size is typically seen. Another option is further evaluation with chemical shift MR imaging utilizing techniques such as in-phase and out-of-phase gradient-echo sequences. Loss of signal on out-of-phase images due to the suppression of fat interspersed between hyperplastic thymic tissue is typically seen. In contrast, thymic epithelial neoplasms, lymphoma, and other soft tissue malignancies do not lose signal on out-of-phase images (25-27) (*Figure 7*).

Thymic epithelial neoplasms
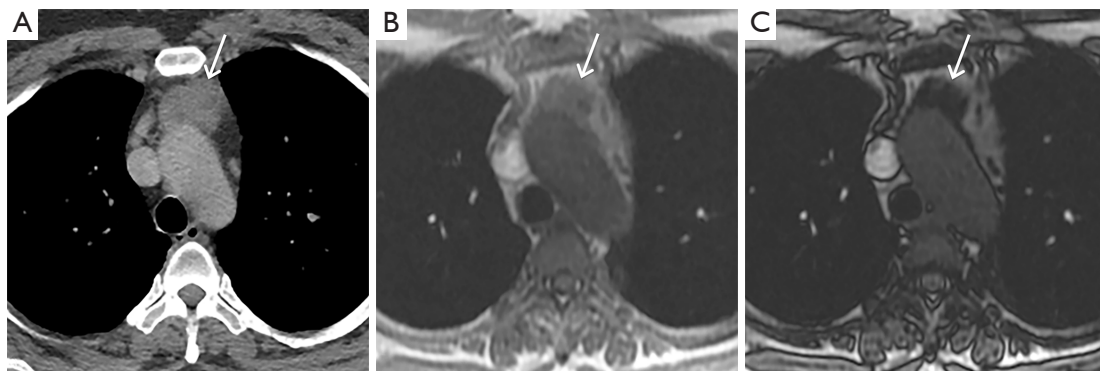Thymic epithelial neoplasms such as thymoma, thymic

Figure 7 Thymic hyperplasia. (A) Contrast-enhanced axial CT of a 38-year-old woman shows a soft tissue mass (arrow) in the prevascular mediastinum. Axial in-phase (B) and out-of-phase MR images (C) of the same patient demonstrate loss of signal intensity on the latter sequence consistent with the presence of microscopic or intravoxel fat in thymic hyperplasia (arrows). Chemical shift MR imaging can be performed to distinguish thymic hyperplasia and normal thymus from other soft tissue masses, as the former lost signal on out-of-phase sequences due to the suppression of microscopic fat interspersed between non-neoplastic thymic tissue but the latter do not. MR, magnetic resonance.
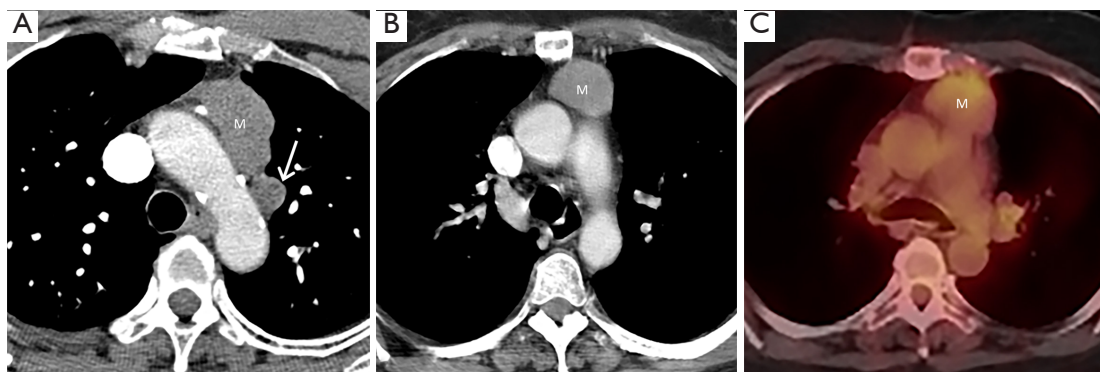
Figure 8 Thymoma. (A) Contrast-enhanced axial CT of a 49-year-old woman with chest pain and myasthenia gravis demonstrates a soft tissue mass [M] in the left prevascular mediastinum consistent with thymoma. Note the adjacent pleural spread of tumor (arrow). In the clinical setting of a prevascular mediastinal mass and a paraneoplastic syndrome such as myasthenia gravis, hypogammaglobulinemia or pure red cell aplasia, thymoma should be suspected. (B,C) Contrast-enhanced axial CT and fused axial FDG PET/CT of a 64-year-old woman shows a focal soft tissue mass [M] in the prevascular mediastinum compatible with thymoma that demonstrates only low-grade FDG uptake. Thymic epithelial neoplasms may demonstrate variable FDG uptake on FDG PET/CT. FDG, fluorodeoxyglucose; positron emission tomography.

carcinoma, and thymic neuroendocrine tumors should be included in the differential diagnosis when a prevascular soft tissue mass is identified on CT. The diagnosis of thymoma should be strongly favored when a homogeneous or slightly heterogeneous mass is present in patients older than 40 years with symptoms related to paraneoplastic conditions such as myasthenia gravis or less commonly pure red cell aplasia/Diamond-Blackfan syndrome, hypogammaglobulinemia, or aplastic anemia (50) (*Figure 8*). Lobulated or irregular contours, internal cystic or necrotic regions, and multifocal calcifications are more suggestive of invasive thymoma than noninvasive thymoma (51,52). Patients may present with advanced disease including spread to the pleura or pericardium, with features such as effusions, thickening, and/or nodules present on imaging (*Figure 8*). However, lymphadenopathy and distant metastases are much less common. Other thymic epithelial neoplasms such as thymic carcinoma and thymic carcinoid should be considered when aggressive features such as greater heterogeneity, local invasion, lymphadenopathy, and/or
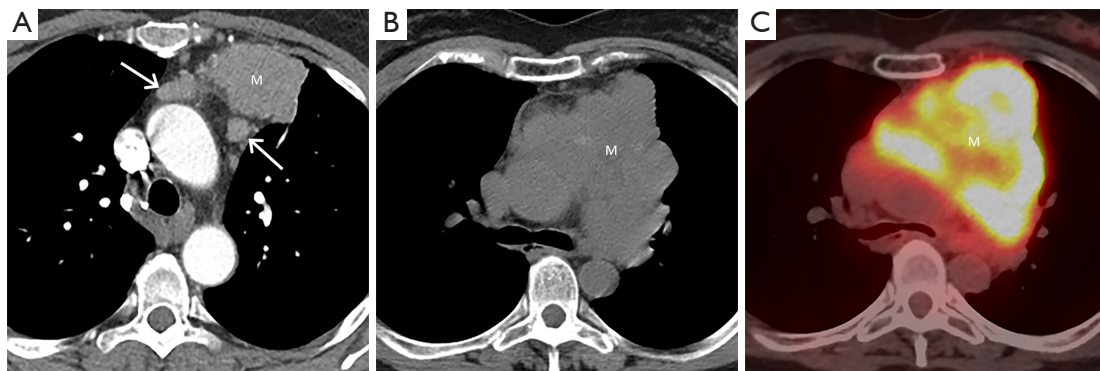
Figure 9 Thymic carcinoma. (A) Contrast-enhanced axial CT of a 58-year-old woman shows a soft tissue mass [M] in the left prevascular mediastinum invading the mediastinal fat. Biopsy revealed thymic carcinoma. Note the multiple enlarged adjacent mediastinal lymph nodes (arrows). In contrast to thymoma, thymic carcinoma and thymic neuroendocrine neoplasms tend to demonstrate aggressive features such as local invasion, intrathoracic lymphadenopathy, and distant metastases. (B,C) Unenhanced axial CT and fused axial FDG PET/CT of a 53-year-old woman shows a large prevascular mass [M] invading the mediastinal fat, ascending thoracic aorta, and left pulmonary artery that is markedly FDG-avid. Although thymic epithelial neoplasms may demonstrate variable FDG uptake on FDG PET/CT, aggressive malignancies such as thymic carcinoma tend to demonstrate greater FDG uptake than others such as thymoma. FDG, fluorodeoxyglucose; positron emission tomography.
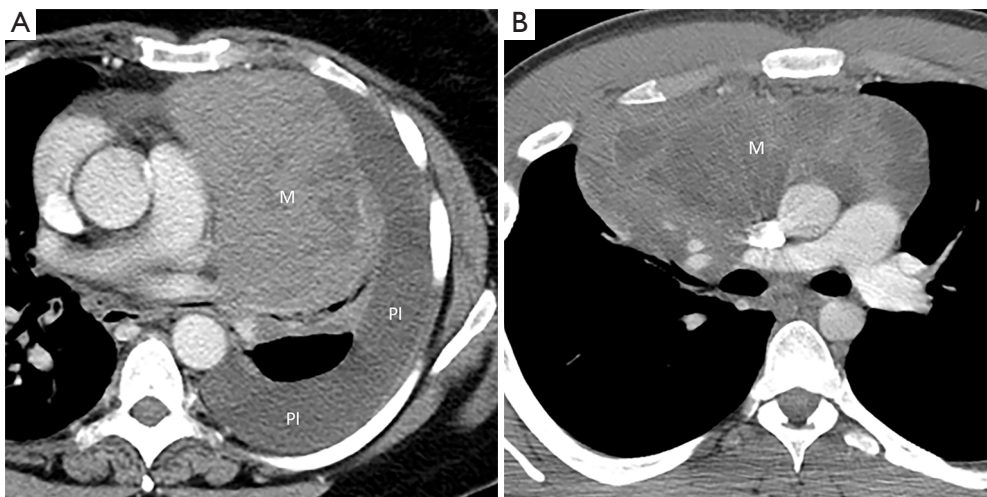

Figure 10 Lymphoma. (A) Contrast-enhanced axial CT of a 45-year-old woman shows a heterogeneous but predominantly low attenuation mass [M] in the left prevascular mediastinum. Biopsy revealed diffuse large B-cell lymphoma. Note the left pleural effusion [Pl]. (B) Contrast-enhanced axial CT of a 20-year-old man with Hodgkin lymphoma demonstrates a heterogeneous mass [M] in the prevascular mediastinum that exerts mass effect on the structures in the visceral compartment.

distant metastasis are present (*Figure 9*).

Lymphoma
Lymphoma should be considered in the differential diagnosis when a large soft tissue mass or a group of enlarged lymph nodes is present in the prevascular

mediastinum on CT, the former of which suggests a primary mediastinal lymphoma and the latter of which suggests secondary disease (*Figure 10*). Primary mediastinal lymphomas include Hodgkin lymphoma and non-Hodgkin lymphomas such as diffuse large B-cell lymphoma, gray zone lymphoma, and T-cell lymphoblastic lymphoma.
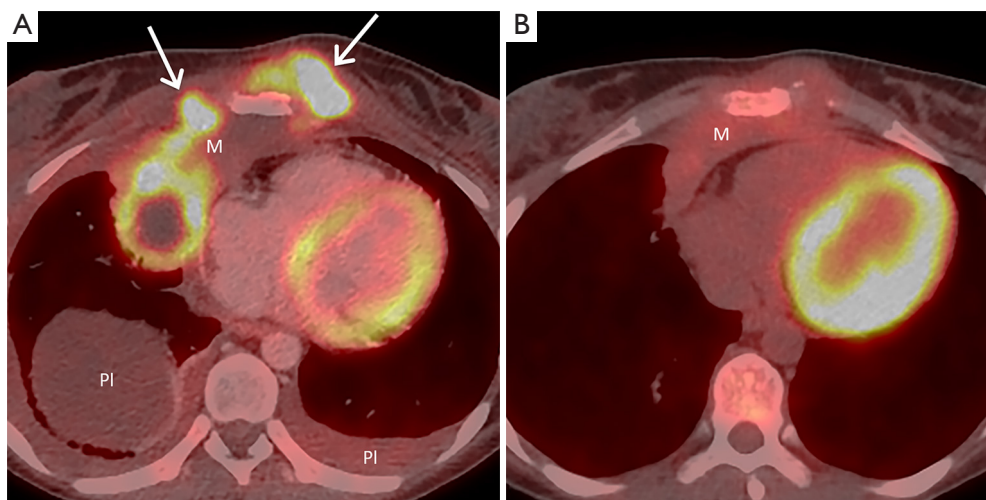
Figure 11 Lymphoma. (A) Staging fused axial FDG PET/CT of a 28-year-old woman with diffuse large B-cell lymphoma demonstrates a large mass [M] in the right prevascular mediastinum that invades the anterior chest wall (arrows). Note the intense FDG uptake in the peripheral aspect of the mass and central low uptake due to necrosis. Small bilateral pleural effusions [Pl] are present. (B) Restaging fused axial FDG PET/CT performed after 1 cycle of chemotherapy demonstrates marked interval decrease in the size of the mass and significant decrease in associated FDG uptake. FDG, fluorodeoxyglucose; positron emission tomography.

One imaging feature that can differentiate mediastinal lymphoma from other neoplasms such as thymic epithelial tumors and germ cell neoplasms is infiltrative growth that can encase or encircle vascular structures without evidence of invasion. These imaging features in combination with clinical information such as "B" symptoms such as fever, weight loss, and night sweats (found in ~50% of cases), the diagnosis can be strongly suggested. Core needle biopsy combined with aspiration for flow cytometry or surgical biopsy are typically performed for diagnosis.

Although the role of FDG PET/CT in the evaluation of mediastinal masses continues to be uncertain, it is the imaging modality of choice for staging and restaging of many types of lymphoma, as well as prognostication, treatment planning, and detecting recurrence (*Figure 11*). Studies have demonstrated that it is more accurate than CT in demonstrating involvement of lymph nodes, with sensitivity of 94% and specificity of 100% compared with 88% and 86%, respectively, for CT, and identifying intranodal and extranodal disease within the body, with sensitivity of 88% and specificity of 100% compared with 50% and 90%, respectively, for CT for detecting end-organ involvement (53). For instance, FDG PET/CT can demonstrate occult lesions in the spleen, gastrointestinal tract, bones, and bone marrow that may not be readily identifiable on CT. It can also be used to guide biopsies and surgeries. It should be noted that some types of lymphoma,

including indolent subtypes of non-Hodgkin lymphoma such as marginal zone and peripheral T-cell lymphomas, may demonstrate little to no FDG uptake (54,55). In these histologic subtypes, a "negative" FDG PET/CT scan does not necessarily exclude disease and complimentary anatomical imaging with CT or MR imaging is necessary. However, FDG PET/CT has shown the ability to detect Richter transformation, characterized by transformation of a low-grade lymphoma to a more aggressive subtype (56).

Nonteratomatous germ cell neoplasms

Nonteratomatous germ cell neoplasms, including seminoma and NSGCTs, should be included in the differential diagnosis when a large prevascular soft tissue mass is present on CT. These lesions may mimic other malignancies in this region; however, a combination of demographic, serologic, and other clinical information can assist in narrowing the differential diagnosis and guiding further management. For example, when a homogeneous mass is present in men 10–39 years of age, seminoma should be suspected (57) (*Figure 12*). Serum levels of certain markers such as b-human chorionic gonadotropin (b-HCG) may be beneficial, as 10% of affected patients demonstrate slightly elevated levels. Although serum levels of lactate dehydrogenase (LDH) are usually elevated in seminoma, this may be seen with other malignancies (58,59). Serum levels of a-fetoprotein (a-FP) levels are typically normal. The diagnosis of mediastinal
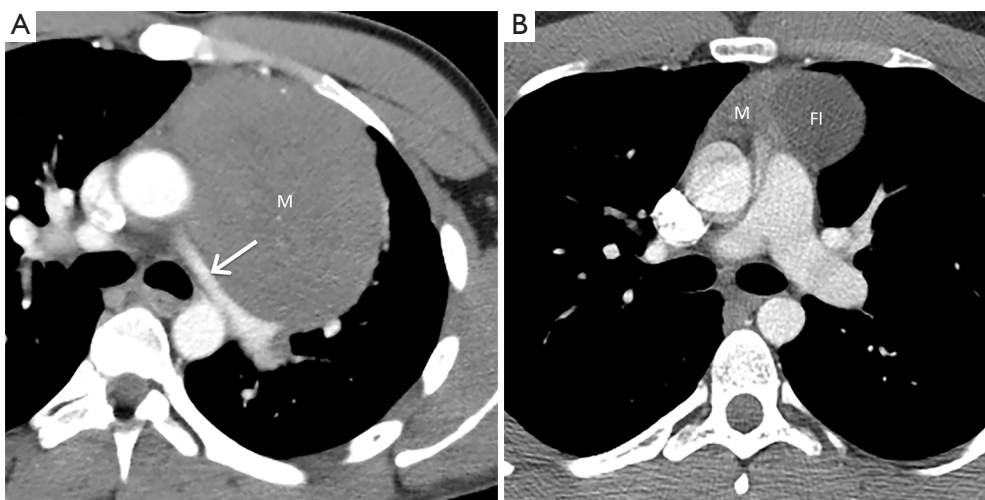
Figure 12 Seminoma. (A) Contrast-enhanced axial CT of a 28-year-old man with elevated serum levels of beta-human chorionic gonadotropin (b-HCG) demonstrates a homogeneous soft tissue mass [M] in the left prevascular mediastinum. Note marked narrowing of the left pulmonary artery (arrow). Biopsy revealed seminoma. Most seminomas affect young men 10–39 years of age and appear as homogeneous soft tissue masses on CT. (B) Contrast-enhanced axial CT of a 24-year-old man performed following chemotherapy demonstrates a soft tissue mass [M] in the prevascular mediastinum and a new region of fluid attenuation [Fl]. Following treatment with chemotherapy, seminomas may develop cystic components.
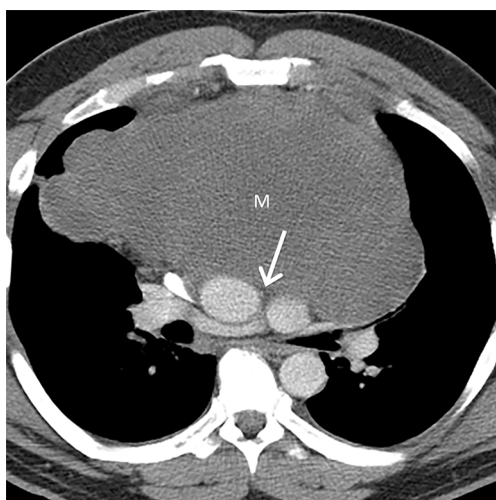

Figure 13 Nonseminomatous germ cell tumor (NSGCT). Contrast-enhanced axial CT of a 34-year-old man shows a large heterogeneous mass [M] arising from the prevascular mediastinum. Note the mass effect exerted on the structures in the visceral compartment (arrow). Compared to seminomas, NSGCTs tend to be larger and more heterogeneous in appearance.

seminoma is usually confirmed with core needle or surgical biopsy. Patients commonly present with evidence of pulmonary metastasis; however, other findings such as pleural spread are rare. Treated lesions may demonstrate cystic components on follow-up examinations (*Figure 12*). NSGCTs should also be considered in men younger than 40 years of age. These malignancies tend to demonstrate greater heterogeneity than other lesions in the prevascular compartment such as seminoma or lymphoma (40,60) (*Figure 13*). In contrast to seminoma, most (90%) patients have markedly elevated serum levels of a-FP or b-HCG at presentation (61,62).

Ectopic parathyroid adenoma
Ectopic parathyroid adenoma should be considered when a soft tissue lesion is present in the prevascular compartment on CT in combination with primary hyperparathyroidism, elevated serum calcium levels and/or elevated serum parathyroid hormone with or without the history of prior parathyroidectomy. Although ectopic parathyroid adenomas are uncommon, the mediastinum is the most frequent involved site (63). Several imaging techniques can be used to evaluate and help diagnose these lesions, including high resolution ultrasonography (US) with color Doppler, technetium 99m (99mTc) sestamibi single photon emission CT (SPECT), CT, and MR imaging. Recently, work has demonstrated that four-dimensional (4D) CT is more sensitive than US and scintigraphy for

the preoperative identification, characterization, and localization of parathyroid adenomas, showing low density on unenhanced CT, intense enhancement in the arterial phase following the administration of IV contrast, and washout of contrast in the delayed phase (64,65). A "polar vessel," defined as an enlarged feeding artery or draining vein, may be identified (66).

Conclusions

Certain masses in the prevascular mediastinum manifest with specific features on CT that enable identification with imaging alone. In other cases, a combination of clinical and imaging information permits a presumptive diagnosis and guides further management. The approach outlined in this article recommends initial inclusion or exclusion of mediastinal abnormalities based on identifiable features on CT and correlation of less conclusive features with clinical information. The new ITMIG classification scheme of mediastinal compartments is designed to enable precise identification of mediastinal abnormalities on advanced imaging techniques such as CT, MR imaging, and FDG PET/CT by radiologists and consistent communication in a multidisciplinary setting.

Acknowledgments

Footnote

Provenance and Peer Review: This article was commissioned by the Guest Editor Mirella Marino for the series "Diagnostic Problems in Anterior Mediastinum Lesions" published in *Mediastinum*. The article has undergone external peer review.

Conflicts of Interest: All authors have completed the ICMJE uniform disclosure form (available at http://dx.doi.org/10.21037/med.2018.12.03). The series "Diagnostic Problems in Anterior Mediastinum Lesions" was commissioned by the editorial office without any funding or sponsorship. BWC and MFB serve as an unpaid editorial board member of *Mediastinum* from May 2017 to Apr 2019. The authors have no other conflicts of interest to declare.

Ethical Statement: The authors are accountable for all aspects of the work in ensuring that questions related to the accuracy or integrity of any part of the work are appropriately investigated and resolved.

References

1. Shields TW. Primary tumors and cysts of the mediastinum. In: Shields TW. editor. General Thoracic Surgery. 3rd ed. Philadelphia: Lea & Febiger, 1983:927-54.
2. Fraser RS, Müller NL, Colman N, et al. The mediastinum. In: Fraser and Paré's Diagnosis of Diseases of the Chest, 4th Ed. Philadelphia, PA: WB Saunders, 1999:196-234.
3. Fraser RG, Paré JA. The normal chest. In: Diagnosis of Diseases of the Chest, 2nd Ed. Philadelphia, PA: WB Saunders, 1977:1-183.
4. Felson B. Chest Roentgenology. Philadelphia, PA: WB Saunders, 1973.
5. Heitzman ER. The Mediastinum. 2nd Ed. New York: Springer-Verlag, 1988.
6. Zylak CJ, Pallie W, Jackson R. Correlative anatomy and computed tomography: a module on the mediastinum. Radiographics 1982;2:555-92.
7. Whitten CR, Khan S, Munneke GJ, et al. A diagnostic approach to mediastinal abnormalities. Radiographics 2007;27:657-71.
8. Aquino SL, Duncan G, Taber KH, et al. Reconciliation of the anatomic, surgical, and radiographic classifications of the mediastinum. J Comput Assist Tomogr 2001;25:489-92.
9. Henschke CI, Lee IJ, Wu N, et al. CT screening for lung cancer: prevalence and incidence of mediastinal masses. Radiology 2006;239:586-90.
10. Carter BW, Okumura M, Detterbeck FC, et al. Approaching the patient with an anterior mediastinal mass: a guide for radiologists. J Thorac Oncol 2014;9:S110-8.
11. Fujimoto K, Hara M, Tomiyama N, et al. Proposal for a new mediastinal compartment classification of transverse plane images according to the Japanese Association for Research on the Thymus (JART) General Rules for the Study of Mediastinal Tumors. Oncol Rep 2014;31:565-72.

12. Carter BW, Tomiyama N, Bhora FY, et al. A modern definition of mediastinal compartments. J Thorac Oncol 2014;9:S97-101.

13. Davis RD Jr, Oldham HN Jr, Sabiston DC Jr. Primary cysts and neoplasms of the mediastinum: recent changes in clinical presentation, methods of diagnosis, management, and results. Ann Thorac Surg 1987;44:229-37.

14. Levasseur P, Kaswin R, Rojas-Miranda A, et al. Profile of surgical tumors of the mediatinum: apropos of a series of 742 operated patients [in French]. Nouv Presse Med 1976;5:2857-9.

15. Cohen AJ, Thompson L, Edwards FH, et al. Primary cysts and tumors of the mediastinum. Ann Thorac Surg 1991;51:378-84; discussion 385-6.

16. Rubush JL, Gardner IR, Boyd WC, et al. Mediastinal tumors: review of 186 cases. J Thorac Cardiovasc Surg 1973;65:216-22.

17. Wychulis AR, Payne WS, Clagett OT, et al Surgical treatment of mediastinal tumors: a 40 year experience. J Thorac Cardiovasc Surg 1971;62:379-92.

18. Mullen B, Richardson JD. Primary anterior mediastinal tumors in children and adults. Ann Thorac Surg 1986;42:338-45.

19. Takeda S, Miyoshi S, Minami M, et al. Clinical spectrum of primary mediastinal tumors: a comparison of adult and pediatric populations. Chest 2000;118:206S.

20. Whooley BP, Urschel JD, Antkowiak JG, et al. Primary tumors of the mediastinum. J Surg Oncol 1999;70:95-9.

21. Azarow KS, Pearl RH, Zurcher R, et al. Primary mediastinal masses: a comparison of adult and pediatric populations. J Thorac Cardiovasc Surg 1993;106:67-72.

22. Tomiyama N, Honda O, Tsubamoto M, et al. Anterior mediastinal tumors: diagnostic accuracy of CT and MRI. Eur J Radiol 2009;69:280-8.

23. Ackman JB, Wu CC. MRI of the thymus. AJR Am J Roentgenol 2011;197:W15-20.

24. Ackman JB. MR imaging of mediastinal masses. Magn Reson Imaging Clin N Am 2015;23:141-64.

25. Carter BW, Benveniste MF, Truong MT, et al. State of the art: MR imaging of thymoma. Magn Reson Imaging Clin N Am 2015;23:165-77.

26. Inaoka T, Takahashi K, Mineta M, et al. Thymic hyperplasia and thymus gland tumors: differentiation with chemical shift MR imaging. Radiology 2007;243:869-76.

27. Takahashi K, Al-Janabi NJ. Computed tomography and magnetic resonance imaging of mediastinal tumors. J Magn Reson Imaging 2010;32:1325-39.

28. Priola AM, Priola SM, Ciccone G, et al. Differentiation of rebound and lymphoidbthymic hyperplasia from anterior mediastinal tumors with dual-echo chemical-shiftbMR imaging in adulthood: reliability of the chemical-shift ratio and signal intensity index. Radiology 2015;274:238-49.

29. Razek AA, Elmorsy A, Elshafey M, et al. Assessment of mediastinal tumors with diffusion-weighted single-shot echo-planar MRI. J Magn Reson Imaging 2009;30:535-40.

30. Benveniste M, Carter BW, Shroff G, et al. Diffusion-weighted MR imaging for assessment of mediastinal masses. Radiological Society of North America Annual Meeting, 11/2016. Available onlin: archive.rsna. org/2016/16004847.html. Accessed May 26, 2019.

31. Sakai S, Murayama S, Soeda H, et al. Differential diagnosis between thymoma and nonthymoma by dynamic MR imaging. Acta Radiol 2002;43:262-8.

32. Jerushalmi J, Frenkel A, Bar-Shalom R, et al. Physiologic thymic uptake of 18F-FDG in children and young adults: a PET/CT evaluation of incidence, patterns, and relationship to treatment. J Nucl Med 2009;50:849-53.

33. Kubota K, Yamada S, Kondo T, et al. PET imaging of primary mediastinal tumours. Br J Cancer 1996;73:882-6.

34. Tatci E, Ozmen O, Dadali Y, et al. The role of FDG PET/CT in evaluation of mediastinal masses and neurogenic tumors of chest wall. Int J Clin Exp Med 2015;8:11146-52.

35. Luzzi L, Campione A, Gorla A, et al. Role of fluorine-flurodeoxyglucose positron emission tomography/computed tomography in preoperative assessment of anterior mediastinal masses. Eur J Cardiothorac Surg 2009;36:475-9.

36. Sung YM, Lee KS, Kim BT, et al. 18F-FDG PET/CT of thymic epithelial tumors: usefulness for distinguishing and staging tumor subgroups. J Nucl Med 2006;47:1628-34.

37. Treglia G, Sadeghi R, Giovanella L, et al. Is (18)F-FDG PET useful in predicting the WHO grade of malignancy in thymic epithelial tumors? A meta-analysis. Lung Cancer 2014;86:5-13.

38. Detterbeck F. Clinical approach to mediastinal masses. In: Kuzdal JML, Muller M, Papagiannopoulos K, et al. editors. ESTS textbook of thoracic surgery. Exeter, England: European Society of Thoracic Surgeons, 2014.

39. Carter BW, Benveniste MF, Madan R, et al. ITMIG Classification of Mediastinal Compartments and Multidisciplinary Approach to Mediastinal Masses. Radiographics 2017;37:413-36.

40. Rosado-de-Christenson ML, Templeton PA, Moran CA. Mediastinal germ cell tumors: radiologic and pathologic correlation. RadioGraphics 1992;12:1013-30.

41. Molinari F, Bankier AA, Eisenberg RL. Fat-containing

lesions in adult thoracic imaging. AJR Am J Roentgenol 2011;197:W795-813.

42. Wright C. Germ cell tumors of the mediastinum. In: Pearson F, Cooper J, Deslauriers J, et al. editors. Thoracic surgery. New York, NY: Churchill Livingstone, 2002;1711-9.

43. Gaerte SC, Meyer CA, Winer-Muram HT, et al. Fat-containing lesions of the chest. RadioGraphics 2002;22:S61-78.

44. Nishino M, Ashiku SK, Kocher ON, et al. The thymus: a comprehensive review. RadioGraphics 2006;26:335-48.

45. Munden RF, Nesbitt JC, Kemp BL, et al. Primary liposarcoma of the mediastinum. AJR Am J Roentgenol 2000;175:1340.

46. Hahn HP, Fletcher CD. Primary mediastinal liposarcoma: clinicopathologic analysis of 24 cases. Am J Surg Pathol 2007;31:1868-74.

47. Nasseri F, Eftekhari F. Clinical and radiologic review of the normal and abnormal thymus: pearls and pitfalls. RadioGraphics 2010;30:413-28.

48. Jeung MY, Gasser B, Gangi A, et al. Imaging of cystic masses of the mediastinum. RadioGraphics 2002;22:S79-93.

49. Kissin CM, Husband JE, Nicholas D, et al. Benign thymic enlargement in adults after chemotherapy: CT demonstration. Radiology 1987;163:67-70.

50. Benveniste MF, Rosado-de-Christenson ML, Sabloff BS, et al. Role of imaging in the diagnosis, staging, and treatment of thymoma. Radiographics. 2011;31:1847-61; discussion 1861-3.

51. Priola AM, Priola SM, Di Franco M, et al. Computed tomography and thymoma: distinctive findings in invasive and noninvasive thymoma and predictive features of recurrence. Radiol Med (Torino) 2010;115:1-21.

52. Tomiyama N, Müller NL, Ellis SJ, et al. Invasive and noninvasive thymoma: distinctive CT features. J Comput Assist Tomogr 2001;25:388-93.

53. Schaefer NG, Hany TF, Taverna C, et al. Non-Hodgkin lymphoma and Hodgkin disease: coregistered FDG PET and CT at staging and restaging—do we need contrast-enhanced CT? Radiology 2004;232:823-9.

54. Tsukamoto N, Kojima M, Hasegawa M, et al. The usefulness of (18)F-fluorodeoxyglucose positron emission tomography ((18)F-FDG-PET) and a comparison of (18) F-FDG-pet with (67)gallium scintigraphy in the evaluation of lymphoma: relation to histologic subtypes based on the World Health Organization classification. Cancer 2007;110:652-9.

55. Elstrom R, Guan L, Baker G, et al. Utility of FDG-PET scanning in lymphoma by WHO classification. Blood 2003;101:3875-6.

56. Bruzzi JF, Macapinlac H, Tsimberidou AM, et al. Detection of Richter's transformation of chronic lymphocytic leukemia by PET/CT. J Nucl Med 2006;47:1267-73.

57. Strollo DC, Rosado-de-Christenson ML. Primary mediastinal malignant germ cell neoplasms: imaging features. Chest Surg Clin N Am 2002;12:645-58.

58. Lemarié E, Assouline PS, Diot P, et al. Primary mediastinal germ cell tumors: results of a French retrospective study. Chest 1992;102:1477-83.

59. Economou JS, Trump DL, Holmes EC, et al. Management of primary germ cell tumors of the mediastinum. J Thorac Cardiovasc Surg 1982;83:643-9.

60. Lee KS, Im JG, Han CH, et al. Malignant primary germ cell tumors of the mediastinum: CT features. AJR Am J Roentgenol 1989;153:947-51.

61. Wright CD, Kesler KA, Nichols CR, et al. Primary mediastinal nonseminomatous germ cell tumors: results of a multimodality approach. J Thorac Cardiovasc Surg 1990;99:210-7.

62. Kesler KA, Rieger KM, Ganjoo KN, et al. Primary mediastinal nonseminomatous germ cell tumors: the influence of postchemotherapy pathology on long-term survival after surgery. J Thorac Cardiovasc Surg 1999;118:692-700.

63. Juanpere S, Cañete N, Ortuño P, et al. A diagnostic approach to the mediastinal masses. Insights Imaging 2013;4:29-52.

64. Rodgers SE, Hunter GJ, Hamberg LM, et al. Improved preoperative planning for directed parathyroidectomy with 4-dimensional computed tomography. Surgery 2006;140:932-40; discussion 940-1.

65. Kukar M, Platz TA, Schaffner TJ, et al. The use of modified four-dimensional computed tomography in patients with primary hyperparathyroidism: an argument for the abandonment of routine sestamibi single-positron emission computed tomography (SPECT). Ann Surg Oncol 2015;22:139-45.

66. Bahl M, Muzaffar M, Vij G, et al. Prevalence of the polar vessel sign in parathyroid adenomas on the arterial phase of 4D CT. AJNR Am J Neuroradiol 2014;35:578-81.